Studies on the dispersion states of Fe_2O_3 on γ-Al_2O_3 by means of Mössbauer spectroscopy and XRD

Youchang Xie, Xianping Xu, Biying Zhao, Youchi Tang
Physical Chemistry Institute, Peking University, Beijing, China

and

Gongbao Wu
Institute of Mineral Geology, Beijing, China

Received 10 July 1991; accepted 15 January 1992

XRD and Mössbauer spectroscopy studies show that Fe_2O_3/γ-Al_2O_3 made by impregnation-calcination method may have monolayer dispersed Fe_2O_3 and α-Fe_2O_3 crystallites. There is a threshold monolayer dispersion capacity. If the Fe_2O_3 loading is lower than the threshold, the Fe_2O_3 will disperse on the surface of γ-Al_2O_3 as a monolayer, then the sample will give an XRD pattern with no crystalline Fe_2O_3 peaks and a Mössbauer spectrum of a doublet with large quadruple splitting (1.11 mm/s). When the Fe_2O_3 loading is higher than the threshold, in addition to the monolayer dispersed Fe_2O_3, crystalline α-Fe_2O_3 will appear, then the sample will give an XRD pattern with crystalline α-Fe_2O_3 peaks and a Mössbauer spectrum with a quadrupole splitting doublet superimposed on a magnetic splitting sextuplet. Monolayer dispersion capacity obtained by quantitative XRD phase analysis and Mössbauer spectra analysis are consistent with each other, having the same value of 0.052 g Fe_2O_3/100 m^2 γ-Al_2O_3 surface.

Keywords: Monolayer dispersion; iron oxide on alumina; Mössbauer spectroscopy

1. Introduction

Supported oxide catalysts are potentially of great industrial significance. The dispersion states of oxides on supports are of importance to catalysis. Supported iron oxide has been studied by Mössbauer spectroscopy [1–7]. It has been reported that Fe_2O_3 supported on γ-Al_2O_3 [4–7] gives Mössbauer spectra of a quadrupole splitting doublet or a magnetic hyperfine splitting sextuplet superimposed on a doublet. The sextuplet is attributed to the bigger α-Fe_2O_3 crystallites which show collective magnetic excitation and the doublet is attributed to the small α-Fe_2O_3 crystallites (e.g. < 100 Å) which show superparamagnetic behaviour due to the fast relaxation of the magnetic moments of the small particles [8,13].

In our previous work, it was found that many oxides and salts can disperse spontaneously onto the surface of supports with high specific surface to form a monolayer or submonolayer [9,10]. For an oxide dispersed on a support, there will be a threshold dispersion capacity. When the content of the oxide on the support is below the threshold, the oxide will be in a monolayer (or submonolayer) dispersion state. If the oxide content exceeds the threshold, the oxide will be present in both the monolayer dispersion state and the crystalline state. According to this point, Fe_2O_3 supported on γ-Al_2O_3 should have both the monolayer (or submonolayer) dispersed Fe_2O_3 and crystalline α-Fe_2O_3. The quadrupole splitting doublet Mössbauer spectra of Fe_2O_3 supported on γ-Al_2O_3 may be mainly contributed from the monolayer dispersed Fe_2O_3 instead of small α-Fe_2O_3 crystallites. The aim of this paper is to prove these predictions, and clarify the states of Fe_2O_3 supported on γ-Al_2O_3.

2. Experimental

γ-Al_2O_3, with B.E.T. surface area of 233 m^2/g, was used as the support. The support was impregnated with a certain amount of 1 N ferric nitrate solution which contains an equivalent oxalic acid to protect the Fe^{3+} ions from hydrolysis in heating. After the impregnation for 3 hours, the precursor was dried under an infrared lamp and calcinated at 500°C for 20 hours to decompose the nitrate and oxalate to get the Fe_2O_3/γ-Al_2O_3 samples.

The Mössbauer adsorption spectra were obtained with an Elscint AME-5 Mössbauer spectrometer. The source was 30 mCi ^{57}Co in a palladium matrix at room temperature and the adsorber was at a temperature ranging from room temperature to liquid nitrogen temperature. The source was moving at a constant acceleration with respect to the adsorber within a velocity range of ± 12 mm/s. The mode of operation was multichannel scaling with 512 recording channels. The baseline counts per channel were $0.5-1.5 \times 10^6$. Powdered sample was mixed with polyethylene powder and put in a thin winder sample box made of lucite. The thickness of the sample was 5–7 mg natural Fe/cm^2. A high purity α-iron foil was used to calibrate the velocity scale and to determine the zero-velocity position.

The XRD phase analysis was carried out on a BD-80 diffractometer with CuKα radiation, Ni filter and a scintillation counter.

3. Results and discussion

XRD study: fig. 1 shows the XRD patterns of the Fe_2O_3/γ-Al_2O_3 samples as well as α-Fe_2O_3 and γ-Al_2O_3. For the sample with low Fe_2O_3 loading (0.053 g

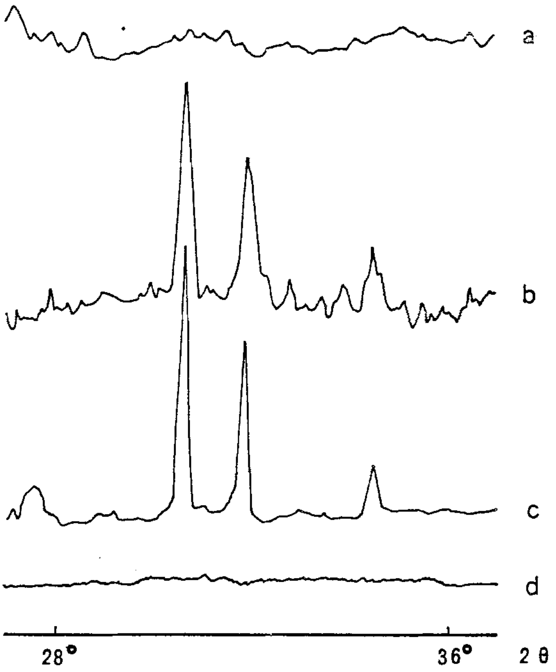

Fig. 1. XRD patterns of $Fe_2O_3/\gamma\text{-}Al_2O_3$ system. (a) 0.053 g Fe_2O_3/g $\gamma\text{-}Al_2O_3$. (b) 0.29 g Fe_2O_3/g $\gamma\text{-}Al_2O_3$. (c) $\alpha\text{-}Fe_2O_3$. (d) $\gamma\text{-}Al_2O_3$.

Fe_2O_3/g $\gamma\text{-}Al_2O_3$), its pattern (fig. 1a) gives no peaks of crystalline $\alpha\text{-}Fe_2O_3$ (see fig. 1c) and is similar to the pattern (fig. 1d) of $\gamma\text{-}Al_2O_3$. It indicates that the Fe_2O_3 disperses on the surface of $\gamma\text{-}Al_2O_3$ as a monolayer [9]. For the sample with higher Fe_2O_3 loading (0.29 g Fe_2O_3/g $\gamma\text{-}Al_2O_3$), its pattern (fig. 1b) has peaks of $\alpha\text{-}Fe_2O_3$. It indicates the presence of the crystalline phase of $\alpha\text{-}Fe_2O_3$ in addition to the monolayer dispersed Fe_2O_3. From the peak area of $\alpha\text{-}Fe_2O_3$ the amount of crystalline $\alpha\text{-}Fe_2O_3$ in the samples can be obtained [11]. Fig. 2 gives the amount of crystalline $\alpha\text{-}Fe_2O_3$ obtained by the XRD quantitative phase analysis as a function of the total amount of Fe_2O_3 in the samples. In the figure, we can find a threshold at 0.12 g Fe_2O_3/g $\gamma\text{-}Al_2O_3$, corresponding to a critical dispersion capacity of 0.052 g Fe_2O_3/100 m^2 $\gamma\text{-}Al_2O_3$ surface. If we assume that the bigger ions, O^{2-}, from Fe_2O_3 form a close-packed layer on the surface of $\gamma\text{-}Al_2O_3$, meanwhile the smaller ions, Fe^{3+}, occupy the interstices formed by O^{2-} ions of Fe_2O_3 and the surface of $\gamma\text{-}Al_2O_3$. By taking the Pauling radius 1.40 Å for the O^{2-} ion, we can get a close-packed monolayer capacity of 0.13 g Fe_2O_3/100 m^2 surface, which is higher than the experimental dispersion capacity of 0.052 g Fe_2O_3/100 m^2 surface of $\gamma\text{-}Al_21O_3$. It indicates that the Fe_2O_3 disperses on the surface of $\gamma\text{-}Al_2O_3$ as a submonolayer. Because the surface sites of $\gamma\text{-}Al_2O_3$ are heterogeneous, it is possible that only a part of the

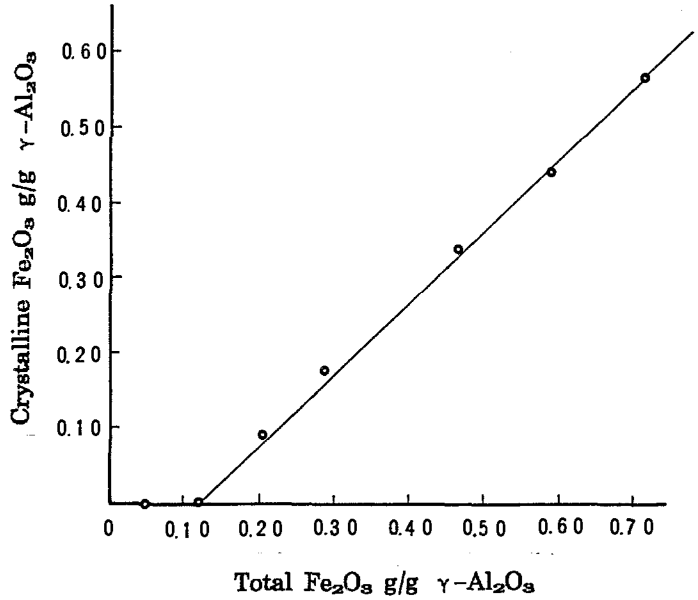

Fig. 2. XRD phase quantitative analysis result of Fe_2O_3/γ-Al_2O_3 system. The threshold is 0.12 g Fe_2O_3/g γ-Al_2O_3.

surface sites are energetically and geometrically favorable for the combination with the ions of Fe_2O_3.

4. Mössbauer spectroscopy study

Fig. 3 shows the Mössbauer spectra of Fe_2O_3/γ-Al_2O_3 samples as well as α-Fe_2O_3 at room temperature. Fig. 3a is a typical magnetic hyperfine splitting sextuplet spectrum of crystalline Fe_2O_3. Fig. 3b is the Mössbauer spectrum of the sample with lower Fe_2O_3 loading (0.053 g Fe_2O_3/g γ-Al_2O_3). It is different from that of the crystalline α-Fe_2O_3 (fig. 3a) and shows a doublet with large quadrupole splitting ($QS = 1.11$ mm/s) and different isomer shift ($IS = 0.33$ mm/s), in comparison with the α-Fe_2O_3 ($IS = 0.38$, $QS = -0.11$ mm/s). The amount of Fe_2O_3 in this sample is below the monolayer dispersion threshold obtained by XRD, so the Fe_2O_3 appears as a monolayer dispersion state. The Fe^{3+} ions on the surface of γ-Al_2O_3 will have a highly asymmetrical environment and feel a strong electric field gradient, therefore give a high quadrupole splitting value ($QS = 1.11$ mm/s) much larger than that of Fe^{3+} in bulk phase α-Fe_2O_3 ($QS = -0.11$ mm/s).

Fig. 3c is the Mössbauer spectrum of a sample with higher Fe_2O_3 loading (0.29 g Fe_2O_3/g γ-Al_2O_3). The amount of supported Fe_2O_3 in the sample is beyond the threshold of monolayer dispersion. So not only monolayer dispersed

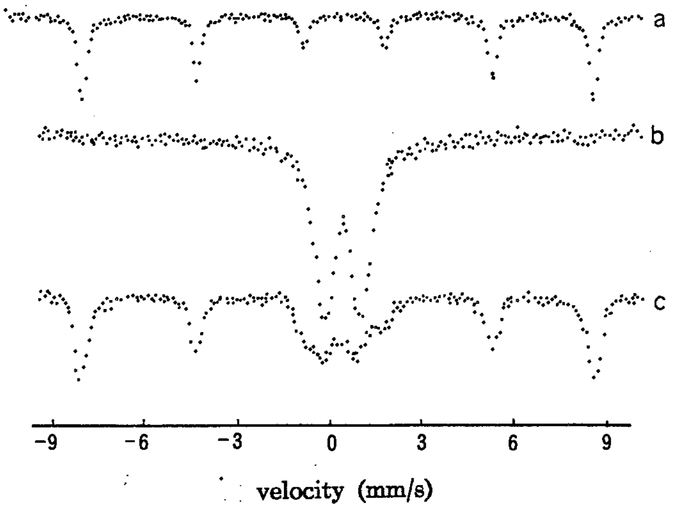

Fig. 3. The Mössbauer spectra of $Fe_2O_3/\gamma\text{-}Al_2O_3$ system. (a) $\alpha\text{-}Fe_2O_3$. $IS = 0.38$ mm/s, $QS = -0.11$ mm/s. (b) 0.053 g Fe_2O_3/g $\gamma\text{-}Al_2O_3$. $IS = 0.33$ mm/s, $QS = 1.11$ mm/s. (c) 0.29 g Fe_2O_3/g $\gamma\text{-}Al_2O_3$.

Fe_2O_3 but also crystalline $\alpha\text{-}Fe_2O_3$ are present in the sample. Its Mössbauer spectrum consists of both doublet with large quadrupole splitting and a magnetic splitting sextuplet.

The relative content of monolayer dispersed Fe_2O_3 and crystalline $\alpha\text{-}Fe_2O_3$ in the sample can be determined from the area of the quadrupole splitting doublet and the magnetic splitting sextuplet. Fig. 4 gives the amount of monolayer dispersed Fe_2O_3 (plot b) and crystalline $\alpha\text{-}Fe_2O_3$ (plot a), respectively as a function of the total Fe_2O_3 in the $Fe_2O_3/\gamma\text{-}Al_2O_3$ samples. Both the plots a and b have turning points at 0.12 g Fe_2O_3/g $\gamma\text{-}Al_2O_3$, corresponding to the monolayer dispersion capacity. It is the same as that obtained by the XRD phase quantitative analysis mentioned above, and strongly supports the monolayer dispersion model.

It has been reported that small $\alpha\text{-}Fe_2O_3$ particles (< 100 Å) can also show only quadrupole splitting spectra at room temperature owing to the superparamagnetism as mentioned before [8,13], but their magnetic splitting sextuplet spectra can appear as the temperature was decreased. So that only the quadrupole splitting doublet appears at room temperature is not enough for proving that the Fe_2O_3 is dispersed in the form of a monolayer. In order to further confirm that the quadrupole splitting doublet comes from the monolayer dispersed Fe_2O_3 instead of small crystallite $\alpha\text{-}Fe_2O_3$, the Mössbauer spectrum of the low loading sample, 0.053 g Fe_2O_3/g $\gamma\text{-}Al_2O_3$, was measured at liquid nitrogen temperature (−195.8°C) and shown in fig. 5b. It is also a doublet similar to the spectrum obtained at room temperature (fig. 5a). Only the signal to noise ratio is improved in the spectrum because the recoilless fractions

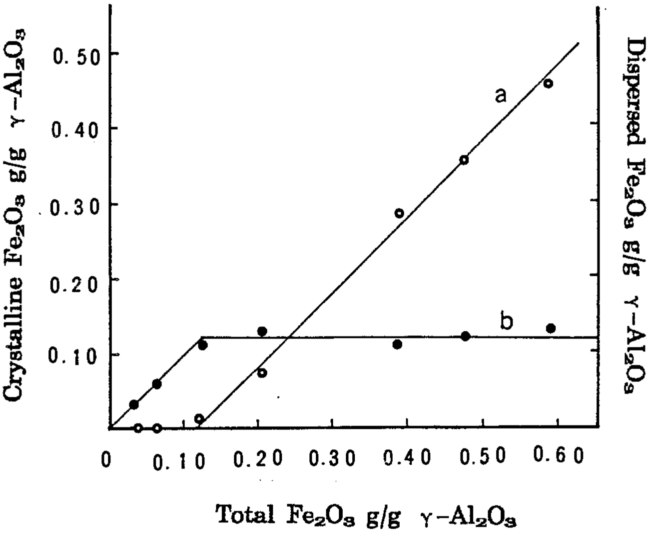

Fig. 4. Mössbauer quantitative analysis results of monolayer dispersed Fe_2O_3 and crystalline α-Fe_2O_3. (a) Relationship between the amount of crystalline α-Fe_2O_3 and total Fe_2O_3. (b) Relationship between the amount of monolayer dispersed Fe_2O_3 and total Fe_2O_3.

become larger when the temperature is lower, but the magnetic hyperfine splitting sextuplet does not appear. It confirms that only monolayer dispersed Fe_2O_3 is present in the sample. We have also measured the Mössbauer spectrum of the sample with higher loading, 0.29 g Fe_2O_3/g γ-Al_2O_3, at liquid

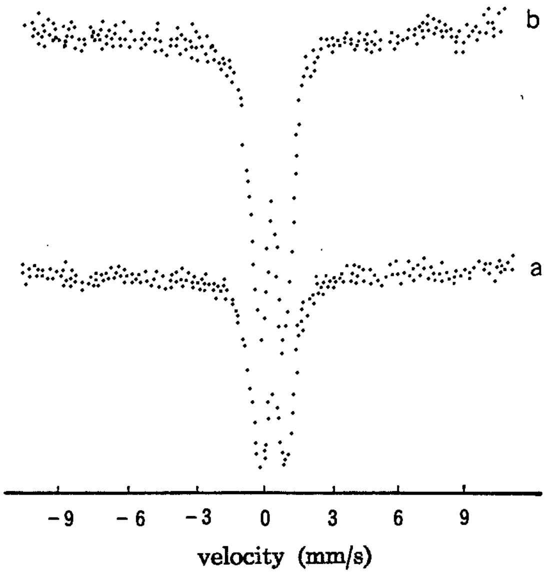

Fig. 5. Mössbauer spectra at room temperature (a), and liquid nitrogen temperature (b), of a sample: 0.053 g Fe_2O_3/g γ-Al_2O_3.

nitrogen temperature, and found that the area ratio of the magnetic splitting sextuplet to the quadrupole splitting doublet was the same as that obtained at room temperature. It confirms the coexistence of both monolayer dispersed Fe_2O_3 and crystalline α-Fe_2O_3 in the sample.

5. Conclusion

The study on Fe_2O_3/γ-Al_2O_3 system by means of XRD and Mössbauer spectroscopy has proved that Fe_2O_3 can disperse on the surface of γ-Al_2O_3 as a monolayer. The monolayer dispersion capacity obtained by Mössbauer and XRD quantitative phase analysis is the same and is 0.052 g $Fe_2O_3/100\ m^2$ γ-Al_2O_3 surface area. When Fe_2O_3 loading is below this threshold, the Fe_2O_3 in the samples will be in a state of monolayer dispersion, and give Mössbauer spectra of a doublet with large quadrupole splitting (1.11 mm/s). When Fe_2O_3 loading exceeds the threshold, the samples will have both the monolayer dispersed Fe_2O_3 and the crystalline α-Fe_2O_3 and give Mössbauer spectra with a quadrupole splitting doublet superimposed on a magnetic splitting sextuplet.

Acknowledgment

The authors acknowledge China's National Natural Science Foundation for generous support of this work.

References

[1] W. Kundig, H. Bommel, G. Constabaris and R.H. Lindquist, Phys. Rev. 142 (1966) 327.
[2] W. Kundig, K.J. Ando, R.H. Lindquist and G. Constabaris, Czech. J. Phys. B17 (1967) 467.
[3] J. Phillips, Y. Chen and J.A. Dumesic, Catal. Characterization Science 43 (1985) 520.
[4] Ding Ying-Ru, Yen Qi-Jie, Hsia Yuan-Fu, Jin Yong-Shu and Qiu Jin-Heng, Mössbauer Spectroscopy and its Applications 29 (1981) 610.
[5] T. Yoshioko, J. Koezuka and H. Ikoma, J. Catal. 16 (1970) 264.
[6] Jr. M.C. Hobson and H.M.J. Gager, J. Catal. 16 (1970) 254.
[7] Sun Yao and Ding Ying-Ru, J. Catal. (Chinese) 5 (1984) 123, 130, 228.
[8] A.M. van de Kraan, Phys. Stat. Sci. 18A (1973) 215.
[9] Xie, Y.C. and Tang, Y.Q., Adv. Catal. 37 (1990) 1.
[10] Xie, Y.C., Yang, N.F., Liu, Y.J. and Tang, Y.Q., Sci. Scin., Ser. B (Chin. Ed.) (1982) 673; Sci. Sin., Ser. B (Engl. Ed) 26 (1983) 337.
[11] Xie, Y.C., Gui, L.L., Liu, Y.J., Zhao, B.Y., Yang, N.F., Guo, Q.L., Duan, L.Y., Huang, H.Z., Cai, X.H. and Tang, Y.Q., in: *Proc. Int. Congr. Catal.*, 8th 5 (1984) 147.
[12] Xie, Y.C., Gui, L.L., Liu, Y.J., Zhang, Y.F., Zhao, B.Y., Yang, N.F., Guo, Q.L., Duan, L.Y., Huang, H.Z., Cai, X.H., and Tang, Y.Q., in: *Adsorption and Catalysis on Oxide Surface*, eds. M. Che and G.C. Bong (Elsevier, Amsterdam, 1985) p. 139.